

Critical Dynamics of Burst Instabilities in the Portevin-Le Châtelier Effect

Gianfranco D'Anna¹ and Franco Nori²

¹ *Institut de Génie Atomique, Ecole Polytechnique Fédérale de Lausanne, CH-1015 Lausanne, Switzerland*

² *Department of Physics, The University of Michigan, Ann Arbor, Michigan 48109-1120*

(February 6, 2008)

We investigate the Portevin-Le Châtelier effect (PLC), by compressing Al-Mg alloys in a very large deformation range, and interpret the results from the viewpoint of phase transitions and critical phenomena. The system undergoes two dynamical phase transitions between intermittent (or “jerky”) and “laminar” plastic dynamic phases. Near these two dynamic critical points, the order parameter $1/\tau$ of the PLC effect exhibits large fluctuations, and “critical slowing down” (i.e., the number τ of bursts, or plastic instabilities, per unit time slows down considerably).

PACS numbers: 62.20.Fe, 81.40.Lm, 83.50.-v

The motion of lattice dislocations is the main source of macroscopic plastic deformation in crystalline solids. In principle, the motion of a single dislocation in an otherwise perfect crystal is a simple phenomenon. However, in a real crystal, many cooperative and core dislocation effects may give rise to unusual and complex plastic properties [1]. An intriguing example of the latter is provided by the Portevin-Le Châtelier (PLC) effect [2], as observed in physical metallurgy (see, e.g., [3,4]). In stress-strain experiments in which the deformation rate is held constant, the stress usually increases monotonically with the strain, and the solid deforms homogeneously in a continuously flowing or “laminar” plastic regime. When the PLC effect arises, notably in some alloys and at high deformation, intermittent yielding points, or *plastic instabilities* are observed, and the deformation is spatially inhomogeneous and apparently confined to mesoscopic channels in the sample. This intermittently flowing or “jerky” plastic regime has been analyzed in terms of microscopic ageing models, which ascribe it to *dislocation-avalanches* triggered by the interaction of dislocations and clouds of mobile impurities [5], or to closely related mechanisms (see, e.g., [3,6]). In these models, mobile point defects are attracted by the stress field of an immobile dislocation, condensing in a cloud around the dislocation. Thus, the pinning force necessary to move the dislocation increases in time and the system ages. By increasing the applied force, and as soon as the stress becomes large enough, the pinning breaks down and the dislocation flashes over a large distance to stop again. This distance is determined by the arrangement of the other dislocations sliding along the same channel and by strong pinning defects. This *cooperative* process repeats itself again and again, producing a succession of plastic instabilities.

Beyond its importance in metallurgy, the PLC effect is a paradigm for a general class of nonlinear complex systems with intermittent bursts. Indeed, the succession of plastic instabilities shares both physical and statistical properties with many other systems exhibiting loading-unloading cycles. This is because the macroscopic statistical properties are a consequence of similar underlying microscopic physical mechanisms (e.g., log-

interacting dislocation lines or magnetic flux lines, slowly driven in a disordered landscape with pinning traps, and obeying glassy dissipative dynamics). Weertman [7], and more recently Lebyodkin *et al.* [8], have analyzed the analogy of the PLC effect with earthquakes. But similarities also exist to stick-slip phenomena in sheared granular media [9], avalanches of magnetic vortices in superconductors [10], “starquakes” with γ -ray burst activity in magnetars [11], and even bursts of economic activity and stock market crashes [12]. The dynamic behavior of some of these systems can be viewed in terms of dynamic phases separated by dynamical critical points (see, e.g., [14] and refs. therein). This is achieved by adapting concepts of equilibrium phase transitions [13] to non-equilibrium cases. It is tempting to extend the analogy to the PLC effect by further studying the dynamics of the jerky regime. Here we present results of compression experiments on 34 polycrystalline Al-Mg samples with nominal 4%Mg. In contrast to the more common traction technique, compression experiments allow to access very large deformations without sample failure, and to collect very long time-series. We interpret our results from the viewpoint of phase transitions and critical phenomena.

Experiments were conducted on 34 samples of the alloy Al-4at.%Mg; a classical system exhibiting the PLC effect [3,8]. Data were collected at room temperature, about 18°C. Samples were slightly oblique cylinders of about 6 mm length and 4 mm diameter, inclined 2 degrees from the vertical; Grain size in the virgin samples was about 100 μm . In Fig. 1 we show a typical segment of a stress versus time curve, for an imposed compression speed $v = 0.18 \mu\text{m/s}$, and when the sample is in the range of a 17% deformation. (The compression velocity is $v = dl/dt$, where l is the actual length of the sample. Deformation is calculated assuming constant volume by $\epsilon = -\ln(1 - \Delta l/l_o)$, where Δl is the elongation and l_o the initial length of the sample [15]). One sees various sequences of elastic reloading of the sample until a yield point is reached, followed by the sharp stress drop typical of the PLC effect. In Fig. 1 we show the negative derivative of the stress versus time, $-d\sigma/dt$. The latter evidences the stress drops as sharp “bursts” of energy

and permits us to clearly define the waiting time τ_n between successive events, and the size s_n of the n th burst. In this way, we also eliminate difficulties related to the small drift of the average stress with the strain hardening, which results in an almost constant offset in $-d\sigma/dt$.

FIG. 1. Short time-sequence, taken in the range of 17% deformation, of the stress σ (and also $-d\sigma/dt$) versus time for an Al-4at.%Mg polycrystalline sample. For all figures, the imposed compression speed v is $0.18 \mu\text{m/s}$, unless otherwise indicated.

FIG. 2. Various $-d\sigma/dt$ versus time for short time-sequences taken from a single measurement over a long time. (a) The first plastic instability appears at about 16% deformation. (b)-(c) The average time τ between successive plastic instabilities diminishes when increasing the deformation. (d)-(e) For large deformations, τ increases and becomes more periodic.

The burst history of a sample is summarized in Fig. 2, which shows five segments of $-d\sigma/dt$ versus time, taken along a single stress versus strain curve measured at constant compression speed $v = 0.18 \mu\text{m/s}$. The first burst appears at about 16% deformation (about 6000 sec after the beginning of the experiment). Above this lower critical deformation, in Fig. 2(a), we observe intense bursts which come in groups of one, two, two, three, and so on. We follow this jerky dynamic regime up to very large deformations. When increasing the deformation, τ_n initially tends to diminish, as the number of events per unit time increases (Fig. 2(b,c)); but beyond about 35% deformation, τ_n tends to increase (Fig. 2(d,e)). At low deformations, below 35%, the sequence of bursts seems random, possibly chaotic [3,16]. For large compressions, the sequence of bursts develops a periodic component (Fig. 2(d,e)). We do not observe here the ‘‘Gutenberg-Richter’’ power law in the distribution of burst sizes, as in ref. [8], but a bell-shaped distribution instead.

The variations of the waiting time τ_n between successive events with the deformation, ϵ_n , is shown in Fig. 3. These data (as well as other measurements in different samples at similar compression speeds) show that τ_n *diverges*, at both low and high deformations, according to power-laws of the form $\tau_n = A_1 (\epsilon_n - \epsilon_{c1})^{-\beta_1}$, and $\tau_n = A_2 (\epsilon_{c2} - \epsilon_n)^{-\beta_2}$. For the divergence at small deformations, we find $\epsilon_{c1}=0.13$ and $\beta_1=0.58$. The second divergence occurs at very large deformations, with $\epsilon_{c2}=1.1$ and $\beta_2=1.8$. In Fig. 3 we show that the system undergoes transitions between jerky and laminar dynamic phases, and exhibits large *fluctuations* and *critical slowing down* in the number of bursts per unit time in the jerky phase close to two non-equilibrium *dynamic critical points*. The divergences are of the form $\tau \propto |\epsilon - \epsilon_{ci}|^{-\beta_i}$; where $t_i = |\epsilon - \epsilon_{ci}|$, ($i = 1, 2$), behave as the analog of the ‘‘reduced temperature’’ for each one of the two phase boundaries separating the different dynamic phases. Surprisingly, the system recovers the laminar plastic flow in

the very large deformation regime.

The effect of the compression speed v on the jerky regime is analyzed in Fig. 4, which shows four segments of $-d\sigma/dt$ versus time, taken at four different compression speeds (in four different samples) at about 25% deformation. By increasing v , the time τ_n between events decreases roughly following a power law. This is shown in Fig. 5, where the local average $\langle \tau_n \rangle \equiv \tau$ is plotted versus v . This average for τ_n is local, in the sense that it is taken over about 30 events around a given deformation. In Fig. 5 we show the local average $\langle \tau_n \rangle$ for 25% and 60% deformation, respectively. Only as a guide to the eye, a power-law ($\tau = Bv^{-\alpha}$) fit to the data is also shown. We find $\alpha \approx 0.8$ at both low and high deformation. Notice that the parameters describing the critical slowing down close to the two dynamic critical points do not seem to be affected by v . For example, for twice the compression velocity v used in Fig. 3, we still obtain two dynamical critical points. One for small deformations, with $\epsilon_{c1}=0.17$ and $\beta_1=0.51$, and a second divergence for very large deformations, with $\epsilon_{c2}=1.07$ and $\beta_2=1.6$.

Fast driving rates and large deformations are almost equivalent in their effect on the PLC dynamics. Fast driving rates push the system into a more periodic-response regime, as do large deformations, while small driving rates favor an aperiodic (possibly random or chaotic) response. A qualitative microscopic explanation can be given. For very small driving rates, the system has time to undergo complex loading-unloading cycles in which a large number of plastic channels are activated and deactivated. At fast driving rates, few percolation-like channels quickly dominate the dynamics and characteristic times appear. Similarly, as the system is squeezed at large deformations, only few channels remain active and the system acquires a periodic response. Similar behavior has been observed in the plastic instabilities and burst-like cooperative motion of ‘‘magnetic flux lines’’ (instead of our ‘‘dislocation lines’’ here) over pinning centers [10].

The revolution in the general understanding of equilibrium critical phenomena was preceded by the gradual realization that apparently dissimilar and unrelated phenomena (e.g., chemical, magnetic, and superfluid transitions) shared some commonalities near critical points. More recently, the focus has shifted to systems far from equilibrium or in metastable or steady states, and to the search for common behaviors and trends near their phase transitions. In our samples, we apply a generalized force, the externally imposed stress, and the samples respond by generating intermittent bursts. This response is quantified by the rate of burst generation, $1/\tau$, which can be seen as the order parameter for the PLC effect; the analog, e.g., of the magnetization M in a magnet, or the density of paired electrons in superconductors. In the PLC effect, the order parameter is a temporal average or ‘‘current’’, the number of bursts per unit time; instead of a spatial average typical for equilibrium systems. Thus,

the order parameter for the PLC dynamic phase behaves as $1/\tau \propto |\epsilon - \epsilon_{ci}|^\beta$, with critical exponent β , as obtained in Fig. 3. The relative deformation, $|\epsilon - \epsilon_{ci}|$, acts as the reduced temperature. In other words, in our samples: $1/\tau \neq 0$ in the jerky PLC phase, and $1/\tau = 0$ in the laminar phase. For magnets: $M \neq 0$ in the ordered ferromagnetic phase, and $M = 0$ in the disordered phase. Microscopic ordering of a spin is induced by the cooperative alignment of the neighboring spins. *Microscopic* motion of a dislocation is induced by the cooperative motion of the neighboring dislocations, in the PLC phase. As clearly seen in Fig. 3, *fluctuations* in the order parameter $1/\tau$ increase near the two dynamic critical points, in analogy with equilibrium phase transitions.

That a *far* from equilibrium transition can be described by an order parameter, is already known for lasers [13]. We add the PLC effect. Like in the PLC effect, a laser is a driven system kept in a stationary state out of equilibrium. When the optical pump power crosses a threshold, a coherent electromagnetic (EM) wave is generated. In a laser, the internal EM field induces order in the form of temporally *correlated* emission events, while random decay events destroy correlations. In our samples, temporally and spatially *correlated* cooperative jump events occur in the PLC phase (e.g., some nearby dislocations jump, while the rest do not move); while many small uncorrelated dislocations move in the laminar phase. Near the critical point, the laser's relaxation time increases. In the PLC effect, also the relaxation time increases—in the sense that the average time τ between bursts increases.

In summary, we have studied the PLC effect in alloys, focusing on its critical behavior near its two dynamical phase boundaries with enhanced fluctuations and diverging relaxation times (i.e., “critical slowing down” of the jerky activity). In the large compression regime, the time between successive plastic instabilities diverges, until finally the jerky regime stops. The discovery of critical behavior in the PLC effect is relevant for the general study of non-equilibrium driven systems with loading-unloading cycles, which produce plastic nonlinear instabilities and complex stick-slip dynamics. We do not know to which extent this dynamic behavior is universal, and if it provides a key for predicting the future evolution of jerky nonlinear systems. However, our findings show an up to now unexplored approach for the PLC, possibly valid for other systems which share similar dynamics, including the seismic activity of crustal faults and the starquakes in the solid crust of superdense stars.

We thank J. Martin and J. Bonneville for providing the testing machines, E. Giacometti for his help in using them, and M. Bretz and C. Kurdak for comments on the text. This work is supported by the Swiss National Science Foundation. FN acknowledges partial support from the UM Center for the Study of Complex Systems,

and DOE contract No. W-31-109-ENG-38.

-
- [1] J. Friedel, *Dislocations* (Pergamon Press, Oxford, 1964); J.P. Hirth and J. Lothe, *Theory of dislocations*, second edition (Wiley, New York, 1982).
 - [2] A. Portevin and F. Le Chatelier, C. R. Acad. Sci. Paris **176**, 507 (1923).
 - [3] Y. Estrin and L.P. Kubin in: H.-B. Mühlhaus (ed), *Continuum models for materials with microstructures* (Wiley, New York, 1995).
 - [4] F. Mertens, S.V. Franklin, and M. Marder, Phys. Rev. Lett. **78**, 4502 (1997).
 - [5] A.H. Cottrell, Phys. Soc. London **30**, (1948); Phil. Mag. **44**, 829 (1953).
 - [6] P. Hähner and M. Zaiser, Acta mater. **45**, 1067 (1997); P.G. McCormick and C.P. Ling, Acta Mater. **43**, 1969 (1995); P. Lukáč, J. Balík and F. Chmelík, Mat. Sci. Eng. **A234-236**, 45 (1997).
 - [7] J. Weertman, Nature **231**, 9 (1971); *Dislocation Based Fracture Mechanics* (W. Scientific, 1996), p. 382.
 - [8] M.A. Lebyodkin *et al.*, Phys. Rev. Lett. **74**, 4758 (1995).
 - [9] B. Miller, C. O'Hern and R.P. Behringer, Phys. Rev. Lett. **77**, 3110 (1996); E. Kolb *et al.*, Eur. Phys. J. B **8**, 483 (1999).
 - [10] S. Field *et al.*, Phys. Rev. Lett. **74**, 1206 (1995); C.J. Olson, C. Reichhardt, F. Nori, Phys. Rev. B **56**, 6175 (97).
 - [11] See, e.g., B. Cheng *et al.* Nature **382**, 518 (1996).
 - [12] D. Sornette, A. Johansen, Physica A **245**, 411 (1997).
 - [13] *Phase Transitions and Critical Phenomena*, 13 volumes, C. Domb, M.S. Green, eds. (Academic, London, 1995).
 - [14] C. Reichhardt, *et al.*, Phys. Rev. B **58**, 6534 (1998); Phys. Rev. Lett. **78**, 2648 (1997); **82**, 414 (1999).
 - [15] J.P. Poirier, Phil. Mag. **26**, 701 (1972).
 - [16] G. Ananthakrishna, C. Fressengeas and L.P. Kubin, Mat. Sci. Eng. **A234-236**, 314 (1997).

FIG. 1. Short time-sequence, taken in the range of 17% deformation, of the stress σ (and also $-\dot{\sigma}$) versus time for an Al-4at.%Mg polycrystalline sample. For all figures, the imposed compression speed v is 0.18 $\mu\text{m/s}$, unless otherwise indicated.

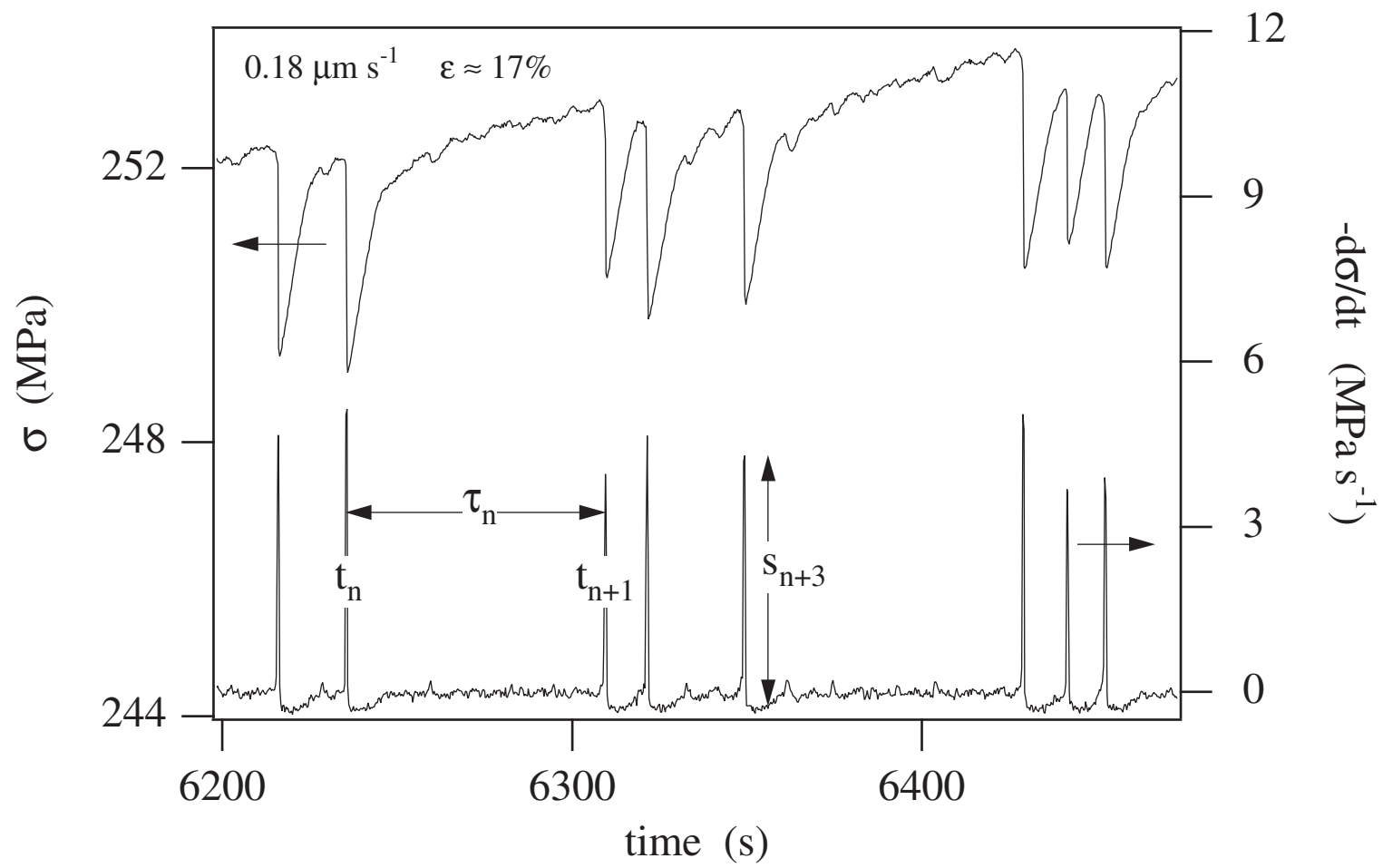
FIG. 2. Various $-\dot{\sigma}$ versus time for short time-sequences taken from a single measurement over a long time. (a) The first plastic instability appears at about 16% deformation. (b)-(c) The average time τ between successive plastic instabilities diminishes when increasing the deformation. (d)-(e) For large deformations, τ increases and becomes more periodic.

FIG. 3. The time τ_n between successive instabilities, versus the deformation, ϵ_n , and power-law fits shown by dashed lines. Large *fluctuations* and *critical slowing down* are evident near the two dynamic critical points.

FIG. 4. Various $-\dot{\sigma}$ versus time for short segments at four different compression speeds v in different samples, at about the same deformation of 25%.

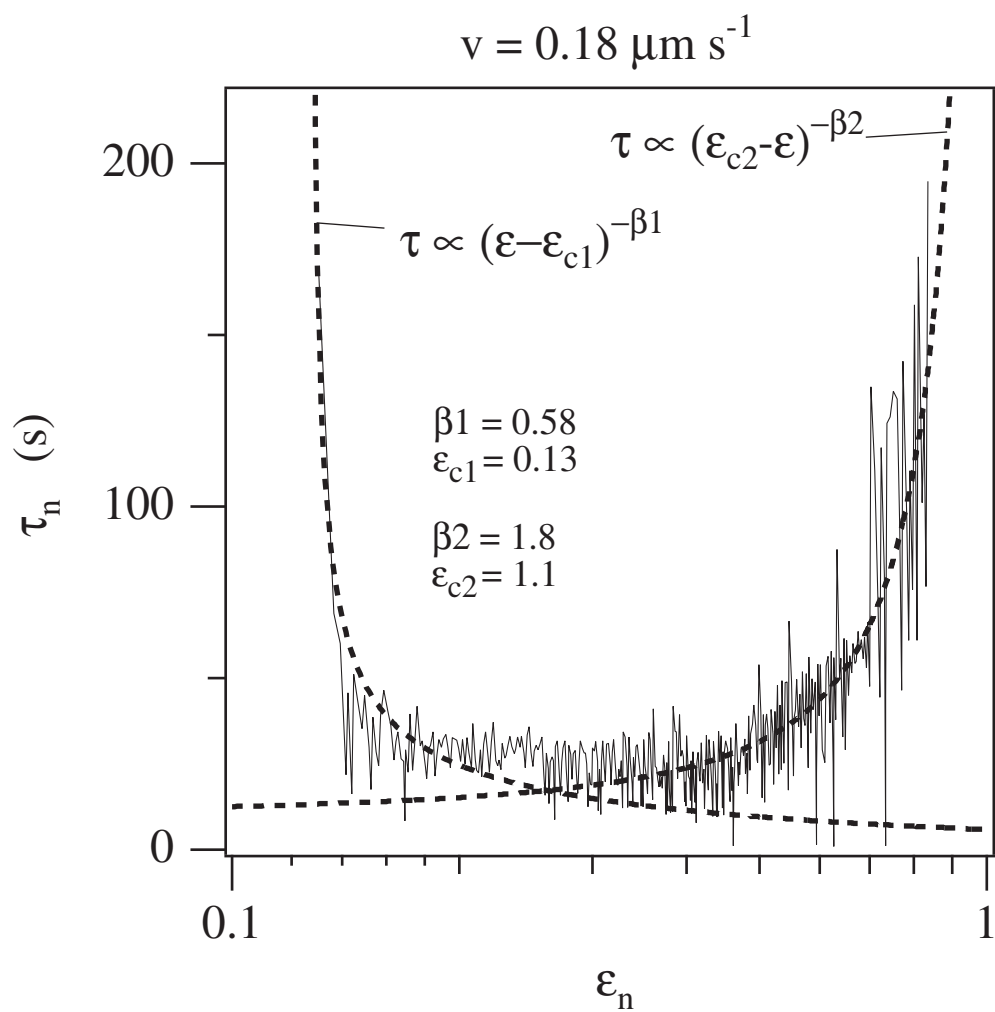
FIG. 5. The average time between bursts versus compression speed v , and power-law fits. These fits have no bearing into the main results (e.g., large fluctuations

and diverging relaxation times, critical slowing down, in the order parameter $1/\tau$ near the two dynamical critical points) because the compressions shown, 25% and 60%, are far from the critical points.



This figure "fig2abc.GIF" is available in "GIF" format from:

<http://arXiv.org/ps/cond-mat/0112010v1>



This figure "plcFig4.gif" is available in "gif" format from:

<http://arXiv.org/ps/cond-mat/0112010v1>

